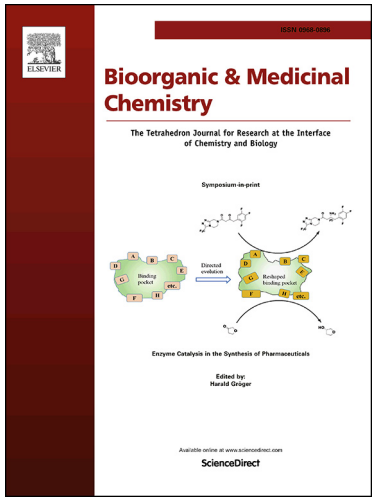

Optimization and Biological Evaluation of Nicotinamide Derivatives as Aurora Kinase Inhibitors

Baohui Qi, Xingwei Xu, Ying Yang, Huan He, Xupeng Yue

PII: S0968-0896(19)30874-0
DOI: https://doi.org/10.1016/j.bmc.2019.07.016
Reference: BMC 15000

To appear in: *Bioorganic & Medicinal Chemistry*

Received Date: 9 June 2019
Revised Date: 2 July 2019
Accepted Date: 4 July 2019

Please cite this article as: Qi, B., Xu, X., Yang, Y., He, H., Yue, X., Optimization and Biological Evaluation of Nicotinamide Derivatives as Aurora Kinase Inhibitors, *Bioorganic & Medicinal Chemistry* (2019), doi: https://doi.org/10.1016/j.bmc.2019.07.016

Optimization and Biological Evaluation of Nicotinamide Derivatives as Aurora Kinase Inhibitors

Baohui Qi*, Xingwei Xu, Ying Yang, Huan He, Xupeng Yue

Department of Bioengineering, Zhuhai Campus of Zunyi Medical University, Zhuhai 519041, Guangdong Province, China

Abstract: Aurora kinases are known to be overexpressed in various solid tumors and implicated in oncogenesis and tumor progression. A series of nicotinamide derivatives were synthesized and their biological activities were evaluated, including kinase inhibitory activity against Aur A and Aur B and *in vitro* antitumor activity against SW620, HT-29, NCI-H1975 and Hela cancer cell lines. In addition, the study of antiproliferation, cytotoxicity and apoptosis was performed meanwhile. As the most potent inhibitor of Aur A, 4-((3-bromo-4-fluorophenyl)amino)-6-chloro-*N*-(4-((6,7-dimethoxyquinolin-4-yl)oxy)-3-fluorophenyl)nicotinamide **(10l)** showed excellent antitumor activity against SW620 and NCI-H1975 with IC_{50} values were 0.61 and 1.06 μM, while the IC_{50} values of reference compound were 3.37 and 6.67 μM, respectively. Furthermore, binding mode studies indicated that compound **10l** forms better interaction with Aur A.

Keywords: Antitumor; Aurora kinases; Kinase inhibitors; nicotinamide; SAR

1. Introduciton

Protein kinases (PKs) catalyzing phosphorylation of serine, threonine, or tyrosine residues of predetermined target proteins are deregulated in numerous diseases [1]. As an important subclass of PKs, Aurora kinase family could phosphorylate serine/threonine amino acid residues and is involved in the regulation of various stages of mitosis, such as centrosome maturation, mitotic

spindle formation, chromosome segregation and cytokinesis during mitosis [2,3].

Aurora kinase family includes three Aurora kinase isoforms designated as Aurora A (Aur A), Aurora B (Aur B) and Aurora C (Aur C), which have quite different and nonoverlapping functions in mitotic processes [4-7]. Aur A plays a pivotal role in centrosome maturation, the mitotic spindle assembly and entry into mitosis [8,9]. Aur B is essential for chromosome condensation, chromosome orientation on the mitotic spindle and the spindle-assembly checkpoint, as well as the final stages of cytokinesis [10,11]. Aur C which appears to have overlapping functions with Aur B during mitotic cell division process is a chromosomal passenger protein [12].

All three Aurora kinases are known to be overexpressed in various solid tumors and implicated in oncogenesis and tumor progression. However, recent study suggested that the sub-type selective Aur A inhibitors might have advantages over pan-selective Aurora kinase inhibitors, by avoiding Aur B-mediated neutropenia [13]. Nevertheless, Aurora kinases have also become promising antitumor targets, and a number of structurally diverse small molecular inhibitors have been reported already, including pyrimidine derivative Tozasertib (VX-680), pyrimidoazepine derivative Alisertib (MLN8237), 3-aminopyrazole derivative Danusertib (PHA-739358), phthalazine derivative AMG900 and quinazoline derivative Barasertib (AZD1152) (Fig. 1) [14-19].

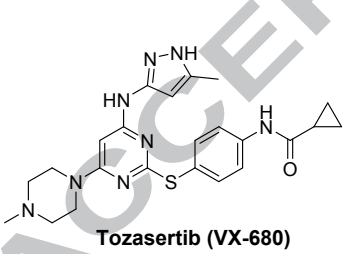

Tozasertib (VX-680)

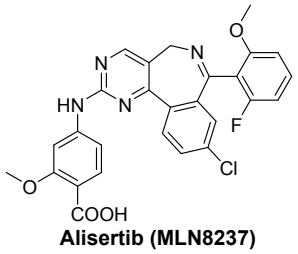

Alisertib (MLN8237)

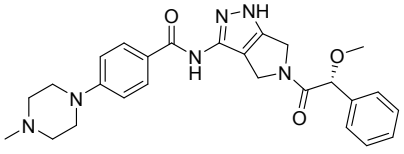

Danusertib (PHA-739358)

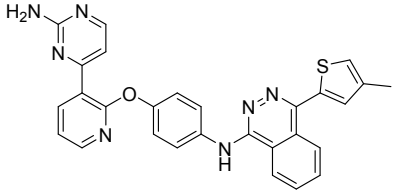

AMG900

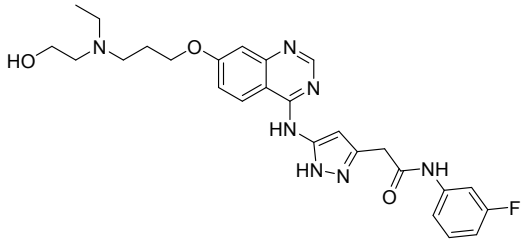

Barasertib (AZD1152)

Fig. 1 The structures of representative Aurora kinase inhibitors.

Nicotinamide and its derivates, known as a scaffold with multiple biological activities, were widely used in drug design, such as tissue-nonspecific alkaline phosphatase (TNAP) inhibitors, acetylcholinesterase inhibitors, psychiatric and neurodegenerative agents, and anticancer agents, etc [20-24]. Based on the structure activity relationship (SAR) of type Ⅱ c-Met inhibitors [25, 26], nicotinamide fragments were introduced into Cabozantinib in our previous work. Unfortunately, the c-Met inhibitory activity of designed compounds was not satisfactory (data not shown). To our delight, their *in vitro* antitumor activity against various cancer cell lines was more potent than that of Cabozantinib. Kinase profile study indicated that they were potent Aurora kinase inhibitors. In this present article, more nicotinamide derivates were synthesized and evaluated for their antitumor activity. In addition, detailed SAR and antitumor mechanism were disclosed concurrently (Fig. 2).

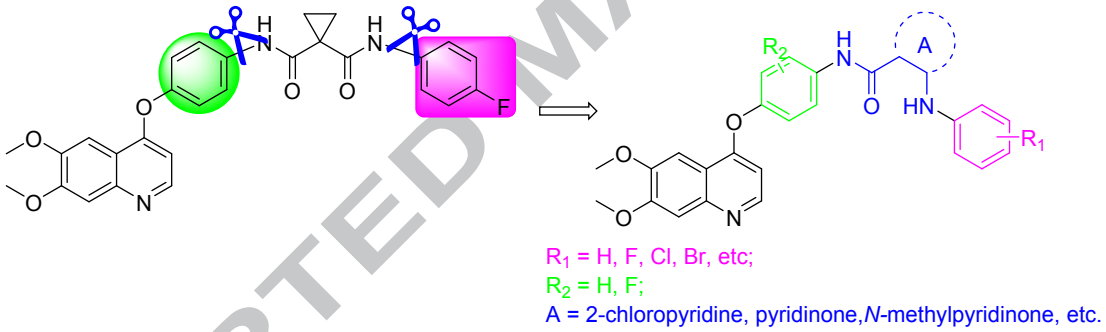

Fig. 2 Design of target compound derived from Cabozantinib.

2. Results and Discussion

2.1. Chemistry

As shown in Scheme 1, selective acid-catalyzed displacement of the 4-chlorine atom of ethyl 4,6-dichloronicotinate with different substituted aromatic amines to yield 4-arylamino-6-chloropyridine esters **1a-k** [27]. The *N*-methylpyridone ester **3** were prepared by quaternization of the ethyl 6-chloro-4-(phenylamino)nicotinate **1a** with dimethylsulfate followed by *in situ* treated with a mixture of AcOH, TEA and EtOH [28]. Hydrolysis of obtained ethyl esters under basic conditions gave the acid **4** which were coupled with amine **8a** by HATU and DIPEA in

DMF to afford target compound **9b** (Scheme 3). The 6-chloro-4-anilinonicotinate **1a** was converted to the desired intermediate **5** by refluxing in AcOH/H_2O [29]. The synthesis of target compounds **9a**, **10a-l** and **11-13** was carried out in a manner similar to that of compound **9b** (Scheme 2 and Scheme 3).

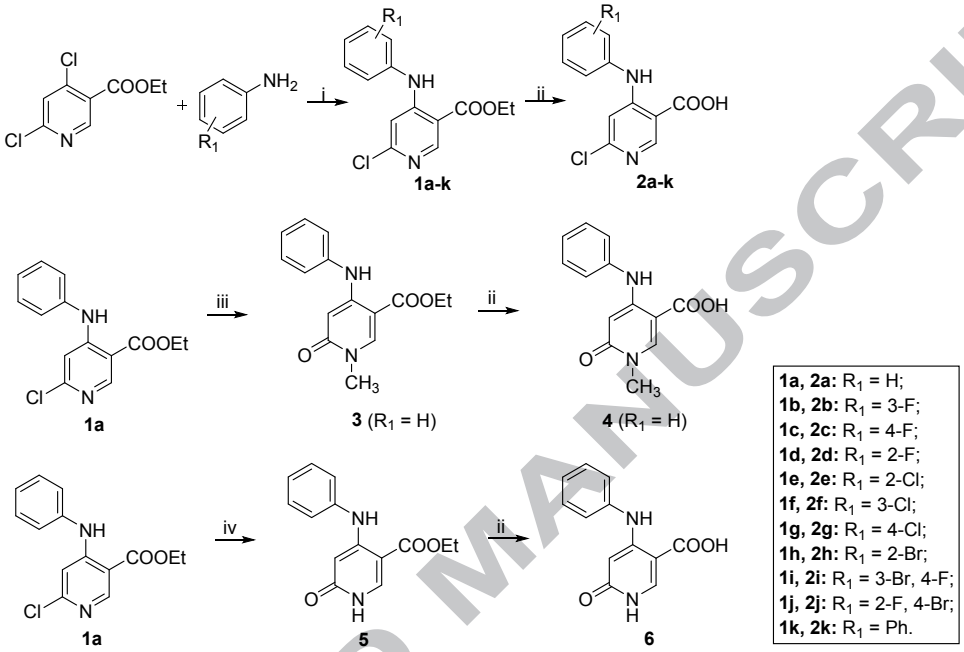

Scheme 1. The synthesis of intermediates **2a-k**, **4** and **6**. Reagents and condition: i) EtOH, concd HCl (cat.), 90 °C, 15 h; ii) NaOH, EtOH, 50 °C, 6 h; iii) a. Me_2SO_4, $CHCl_3$, 0 °C to reflux, b. TEA, AcOH, EtOH, reflux 4 h; iv) AcOH, H_2O, reflux, 48 h.

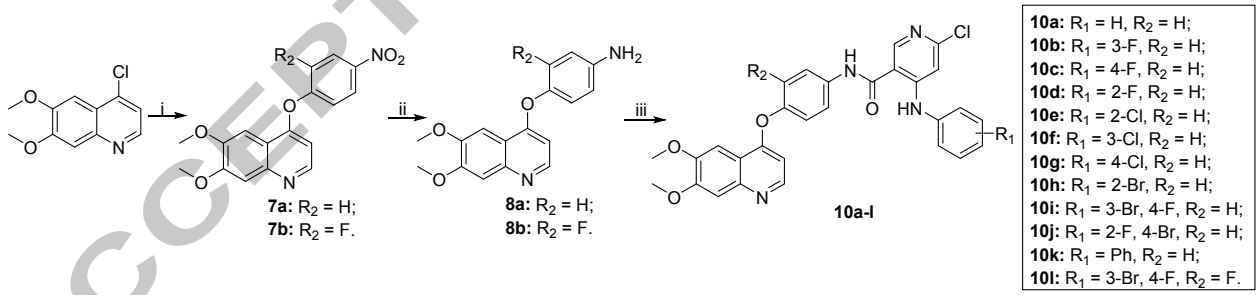

Scheme 2. The synthesis of intermediates**10a-l**. Reagents and condition: i) 4-nitrophenol or 2-fluoro-4-nitrophenol, PhCl, DIPEA, reflux, 13 h; ii) Fe, 90% EtOH-H_2O, AcOH, reflux, 4 h; iii) **2a-k**, HATU, DIPEA, DMF, rt, 2 h.

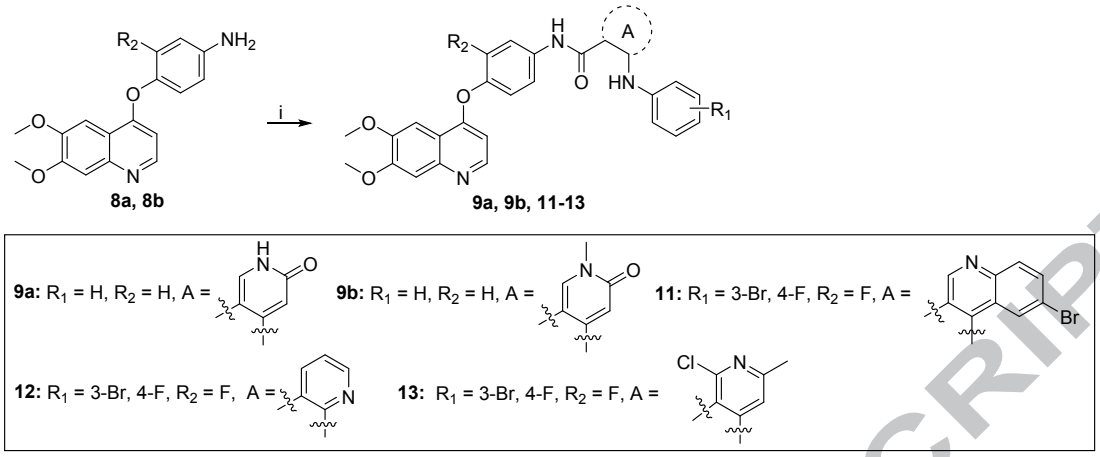

Scheme 3. The synthesis of intermediates **9a-b** and **11-13**. Reagents and condition: i) **4,6** or carboxylic acid;, HATU, DIPEA, DMF, rt, 2 h.

2.2. Biological evaluation and Structure activity relationship

Taking Cabozantinib as reference compound, *in vitro* kinase assay was performed at a single-dose concentration of 0.2 μM over Aur A and Aur B by mobility shift assay. *In vitro* antitumor activity against SW620, a cancer cell line usually used in the study of developing Aurora kinase inhibitors, was identified by MTT assay (Table 1). In general, four compounds (**10h-j** and **10l**) showed high potency over 70% inhibitory rate against Aur A, and most of these compounds were less inhibitive against Aur B (13.7−57.1% inhibition at 0.2 μM).

Preliminary modification of the ring A was carried on by introducing 2-pyridinone **9a**, *N*-methylpyridinone **9b** and 2-chloropyridine **10a** into the target compounds. As can be seen in Table 1, **10a** exhibited more potent kinase inhibitory activity and cellular activity among the three compounds. Therefore, more 2-chloropyridine derivates **10b-l** were synthesized and evaluated for their biological activity in order to disclose the influence of R_1 substitutions on terminal phenyl ring. The biological results indicated that halo substituted phenyl ring led to better activity, especially in *o*- or *m*-position. In comparison with fluoro and chloro analogues **10b-g**, bromo analogues **10h-j** showed a considerable improvement in both kinase inhibitory activity and cellular activity.

Modification came to the central benzyl ring (R_2) in the following work. As shown in table 1, incorporation of fluorine led to over 2-fold improved antitumor activity and slightly increase in Aur A inhibitory potency (**10l** vs **10i**).

With these preferred groups at R_1 (R_1 = 3-Br, 4-F) and R_2 (R_2 = F) in place, additional structural variations were introduced to the heterocyclic core A. The Aur A potency drastically declined due to the replacing of 2-chloropyridine **10l** with 6-bromoquinoline **11** or 2-chloro-6-methylpyridine **13,** suggesting that incorporation of bulky groups in ring A was unprofitable.

Table 1. Enzyme inhibitory activity and *in vitro* antitumor activity against human colon cancer cell SW620.

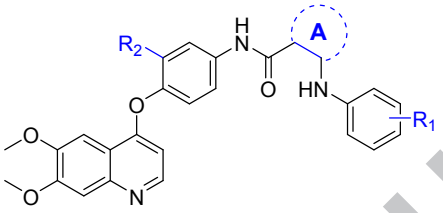

Compd.	A	R_1	R_2	Inh@0.2 μM (%)[a]		SW620
				Aur A	Aur B	IC_{50} (μM)[b]
9a	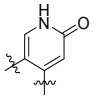	H	H	29.9	38.7	18.9 ± 1.95
9b	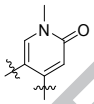	H	H	40.9	31.1	4.43 ± 0.42
10a		H	H	48.2	52.1	1.92 ± 0.18
10b		3-F	H	48.6	49.6	5.10 ± 0.46
10c		4-F	H	47.1	51.6	6.82 ± 0.55
10d		2-F	H	51.5	50.1	8.10 ± 0.76
10e		2-Cl	H	68.3	57.1	3.60 ± 0.31
10f		3-Cl	H	55.1	31.9	4.33 ± 0.42
10g		4-Cl	H	51.9	38.5	2.38 ± 0.21
10h		2-Br	H	78.2	56.1	6.90 ± 0.62

10i		3-Br, 4-F	H	81.3	30.1	1.33 ± 0.12
10j		2-F, 4-Br	H	70.0	31.6	2.45 ± 0.20
10k		Ph	H	59.9	46.3	ND[c]
10l		3-Br, 4-F	F	82.9	30.5	0.61 ± 0.046
11	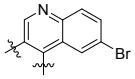	3-Br, 4-F	F	6.6	13.7	ND
12		3-Br, 4-F	F	48.4	40.7	1.86 ± 0.16
13	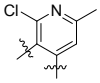	3-Br, 4-F	F	0.6	17.7	ND
Cabozantinib	-	-	-	0.4	38.3	3.37 ± 0.31

a)The results are mean values of two independent determinations. b) The values were an average of three separate determinations and standard deviations were shown. c) Not determined.

In order to further study of *in vitro* antitumor activity, more potent compounds **10h**, **10i**, **10j** and **10l** were selected and the *in vitro* antitumor activity against HT-29, NCI-H1975 and Hela cancer cell lines were evaluated. Generally, all the four compounds exhibited less antitumor activity against HT-29, NCI-H1975 and Hela compared with that of SW620 (Table 2). Compound **10l** showed acceptable activity against NCI-H1975 cell lines with IC_{50} of 1.06 μM which was approximate 6-fold more potent than that of Cabozantinib (IC_{50} = 6.67 μM).

Table 2. *In vitro* antitumor activity of selected compounds against HT-29, NCI-H1975 and Hela cancer cell lines.

Compd.	**IC_{50} (μM)[a]**		
	HT-29	**NCI-H1975**	**Hela**
10h	>20	8.00 ± 0.67	>20
10i	>20	3.54 ± 0.29	>20
10j	>20	ND[b]	>20
10l	>20	1.06 ± 0.09	>20

Cabozantinib	9.6 ± 0.74	6.67 ± 0.58	>20

a) The values were an average of three separate determinations and standard deviations were shown. b) Not determined.

2.3. Effects on proliferation

IncuCyte live-cell imaging assay was carried on to evaluate whether potent compound **10i** and **10l** could inhibit proliferation of cancer cell. As shown in **Fig. 3** and **Fig. 4**, similar inhibition in cancer cell proliferation was induced by compound **10i** (confluence 42.6%) and Cabozantinib (confluence 40.9%) at the concentration of 10.0 μg/mL. However, compound **10l** showed less antiproliferative activity at the same concentration. Lower concentrations (3.33, 1.11, 0.37 and 0.12 μg/mL) of compounds **10i**, **10l** and Cabozantinib could not induce antiproliferative activity significantly (data not shown).

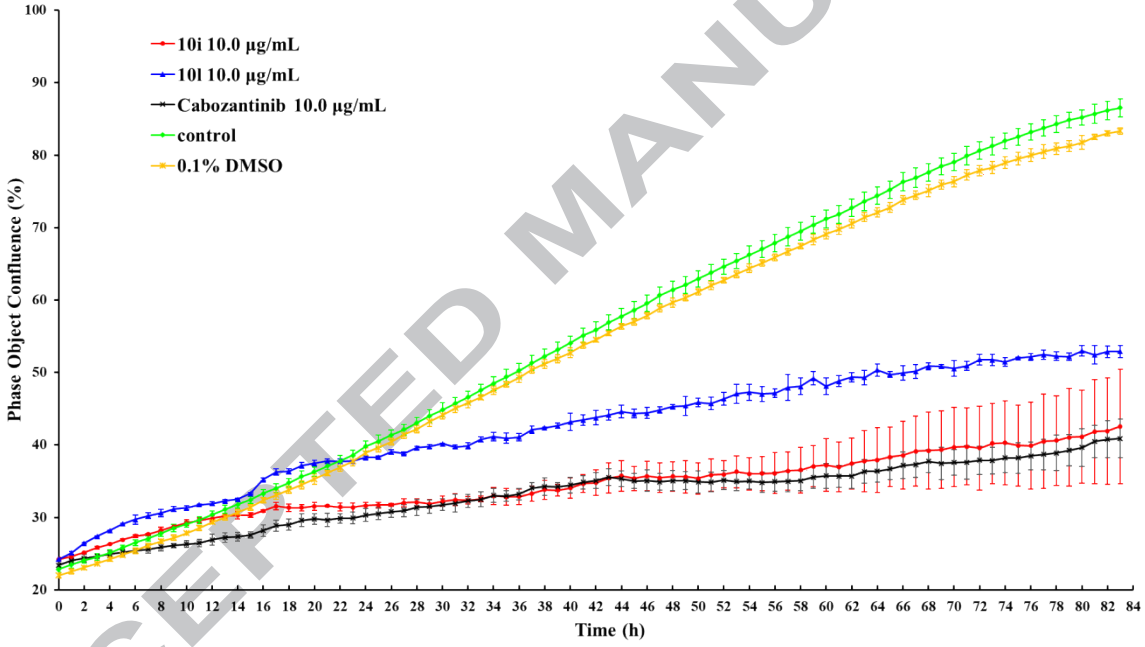

Fig. 3 The curves of antiproliferative activity against SW620 cancer cells. The cell confluence was monitored for 84 h using an IncuCyte ZOOM system in an incubator. SW620 cancer cells were incubated with 0.1% DMSO or exposed to compound **10i**, **10l** or Cabozantinib at different concentration.

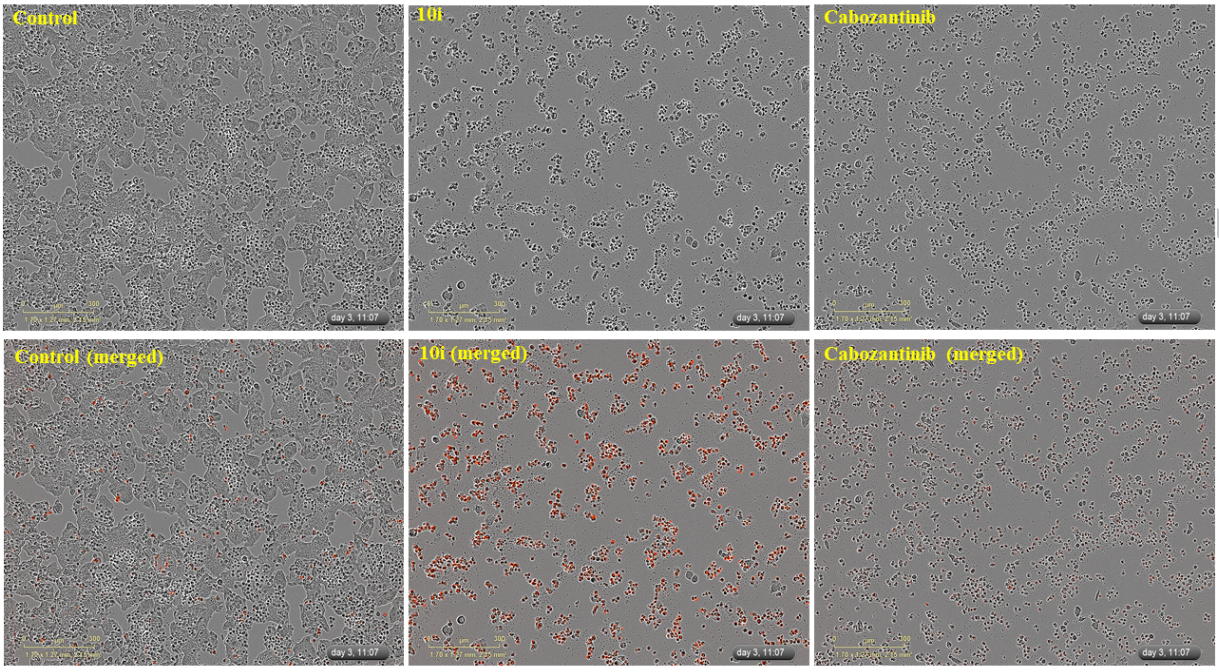

Fig. 4 Phase contrast images (white light) of SW620 cancer cells after 84 h of treatment with Cabozantinib (10.0 μg/mL), compound **10i** (10.0 μg/mL) or not (control). The confluence was 86.5% in control group. Red fluorescent cells were counted as dead cell.

2.4. Effects on cytotoxicity

In order to compare the effects of target compounds and Cabozantinib upon the kinetics of cytotoxicity against SW620 cell line, compounds **10i** and **10l** were selected and real-time IncuCyte live-cell imaging assay was performed. In general, both compounds showed more excellent cytotoxicity than that of Cabozantinib in a dose- and time-dependent manner (Fig. 5). As can be seen in Fig. 5 and Fig. 6, significant cytotoxicity was emerged after being treated with compound **10l** (10.0 μg/mL) for 5 hours, and the number of dead cells reached the maximum at approximate 36 h.

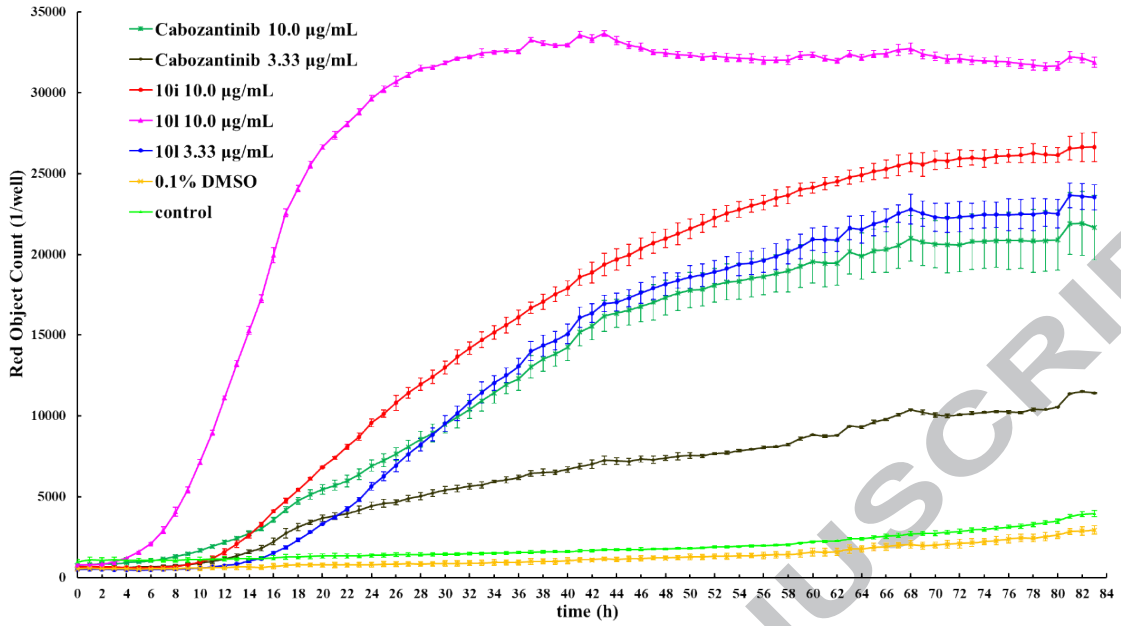

Fig. 5 The kinetics of cytotoxicity study in SW620 cancer cells. The number of dead cells was being monitored for 84 h using an IncuCyte ZOOM system in an incubator. SW620 cancer cells were incubated with 0.1% DMSO or exposed to compound **10i**, **10l** or Cabozantinib at different concentration.

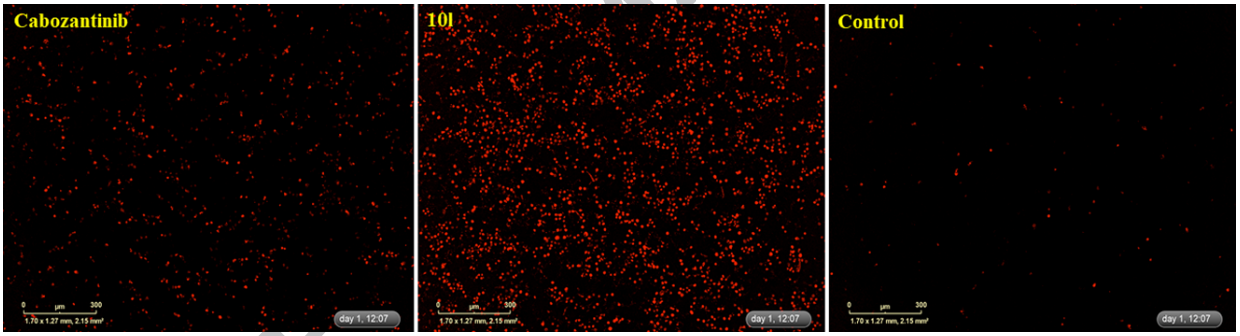

Fig. 6 The images (red light) of study on cytotoxicity against SW620 cancer cells after treatment with compound **10l** (10.0 μg/mL), Cabozantinib (10.0 μg/mL) or not (control) for 36 h. Red fluorescent cells were counted as dead cells.

2.5. Effects on Apoptosis

In comparison with compound **10i** and Cabozantinib, the number of apoptotic cells was significantly increased from 7 h to 24 h after being treated with compound **10l** (10.0 μg/mL). Lower concentration (3.33 μg/mL) resulted in a loss of potency in apoptosis. These results indicated that target compounds induced apoptosis in a time- and dose-dependent manner in SW620 cancer cells.

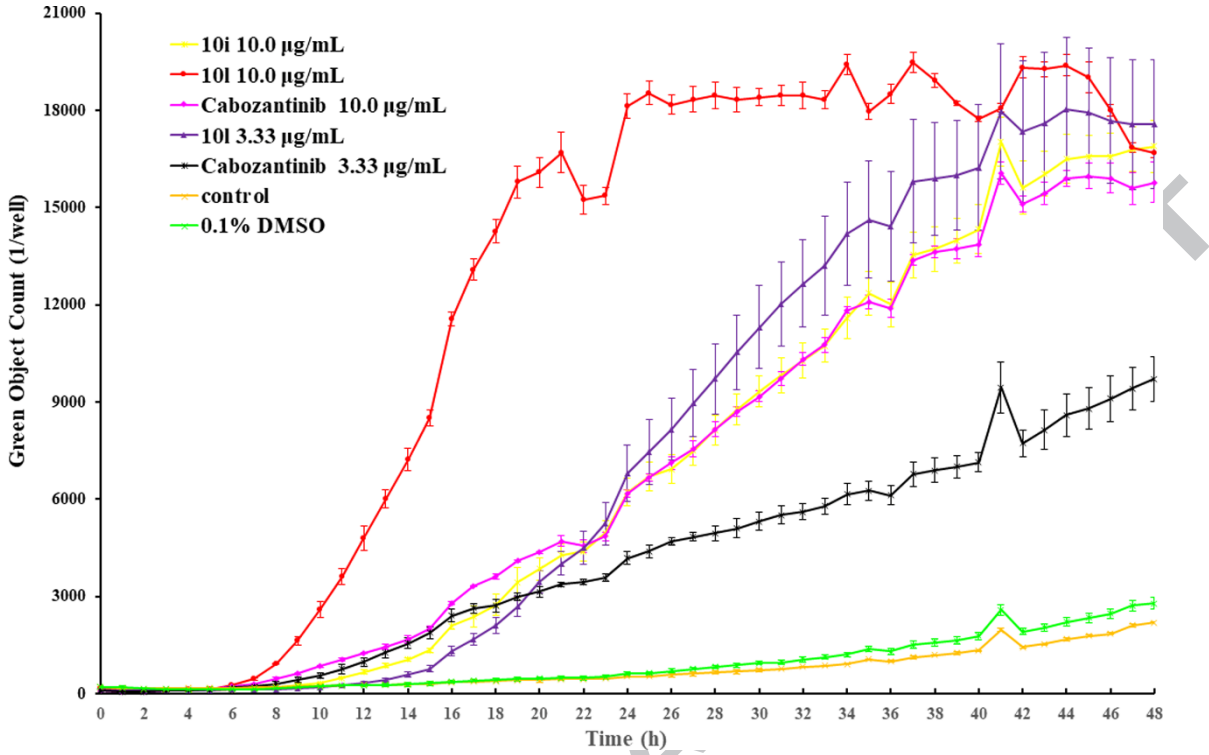

Fig. 7 The kinetic study of apoptosis in SW620 cancer cells. Apoptotic cell death was being monitored for 48 h using an IncuCyte ZOOM system in an incubator. SW620 cancer cells were incubated with 0.1% DMSO or exposed to compound **10i**, **10l** or Cabozantinib at different concentration.

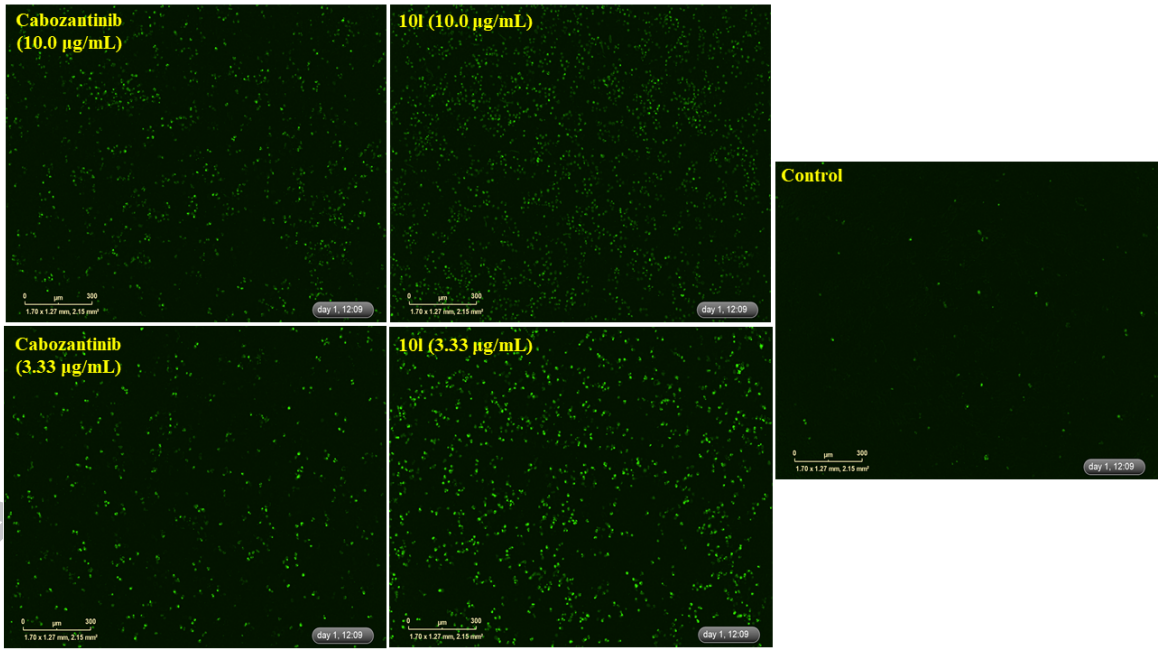

Fig. 8 The images (green light) of study on apoptosis against SW620 cancer cells after treatment with compound **10l** (10.0 and 3.33 µg/mL), Cabozantinib (10.0 and 3.33 µg/mL) or not (control) for 36 h. Green fluorescent cells were counted as dead cells induced by apoptosis.

2.6. Docking study

In order to determine the binding mode of this series of inhibitors, the most potent compound **10l** was selected and molecular docking analysis was performed by Molecular Operating Environment (MOE, Chemical Computing Group Inc., Canada). The binding results indicated that compound **10l** occupies the ATP-binding site with the activation loop in a DFG-in conformation (Fig. 9B and 9D). Three H-bonds could be found in the binding mode: one was established between the quinoline scaffold and Ala213 in the hinge region of the kinase, another was between the NH (PhNH-) and Asp274, a third was between NH (-NHCO-) and Asp274 (Fig. 9C and 9D). In addition, the binding affinity was strengthened by arene-H interaction between quinoline and Leu139. These key interactions might contribute to the high *in vitro* potency of compound **10l**.

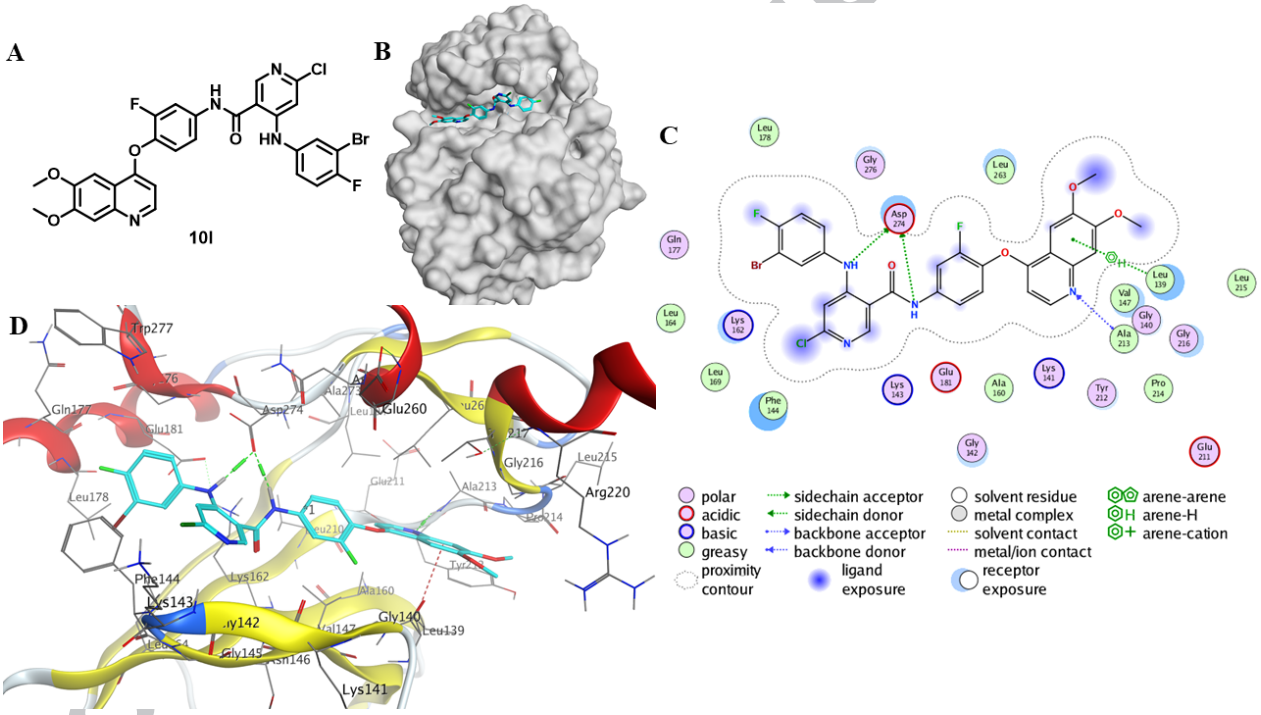

Fig. 9 Docked binding modes of compound **10l** with Aur A (PDB entry 2X6D). The compound was shown by blue sticks, the H-bonds were represented by green dotted lines, and the arene-H and interaction were shown by red dotted lines.

3. Experimental

3.1. Chemistry

Unless otherwise noted, all materials were obtained from commercial suppliers and used without further purification. ^{1}H NMR and ^{13}C NMR spectra were generated on Bruker ARX-400

and Bruker ARX-100 spectrometers (Bruker Bioscience, Billerica, MA, USA). Column chromatography was carried out on silica gel (200-300 mesh). High Resolution Mass spectra (HRMS) were taken in ESI mode on Agilent 6520 LC-HRMS (Agilent, Palo Alto, CA, USA).

3.1.1. Ethyl 6-chloro-4-(phenylamino)nicotinate **(1a)**

To a stirred a solution of ethyl 4,6-dichloronicotinate (2.0 g, 9.1 mmol) in EtOH (30 mL), aniline (0.91 g, 10.0 mmol) and 2 drops of concd HCl were added. The mixture was refluxed for 16 h, and then the solution was cooled, whereupon the desired product crystallized out of solution. The product was filtrated and washed with cold EtOH to give desired compound as white solid (1.2 g, 47.2%). HRMS (ESI) m/z: 277.0703 $[M+H]^+$, calcd. for 277.0744.

Taking different aromatic amines as starting materials, intermediates **1b-k** were prepared by the same procedure as **1a**.

3.1.2. 6-Chloro-4-(phenylamino)nicotinic acid **(2a)**

A solution of NaOH (0.52 g, 12.9 mmol) in water (20 mL) was added to the mixture of **1a** (1.2 g, 4.3 mmol) in EtOH (24 mL), and the suspension was stirred for 5 h at 50 ℃. EtOH was evaporated under reduced pressure, the pH was adjusted to 3 with diluted HCl, and the solid residue obtained was filtered to afford **2a** (0.92, 86.3%). ^{1}HNMR (400 MHz, DMSO-d_6) δ 9.46 (s, 1H), 8.15 (s, 1 H), 7.29-7.34 (m, 4H), 7.21-7.25 (m, 1H), 6.91 (s, 1H). HRMS (ESI) m/z: 247.0235 $[M-H]^-$, calcd. for 247.0274.

Intermediates **2b-k**, **4** and **6** were prepared by the same procedure as **2a**.

3.1.3. Ethyl 1-methyl-6-oxo-4-(phenylamino)-1,6-dihydropyridine-3-carboxylate **(3)**

To a solution of intermediate **1a** (1.0 g, 3.6 mmol) in $CHCl_3$ (25 mL), dimethyl sulfate (2.0 mL, 21.6 mmol) was added dropwise at 0 ℃.The solution was allowed to warm to rt and then heated at reflux for 18 h. After cooling to rt, a mixture of triethylamine (10.6 mL), acetic acid (7.1 mL), and EtOH (7.1 mL) was added and the reaction heated at reflux for a further 3 h. Water (60 mL) was added and the mixture was extracted with ethyl acetate (3×30 mL). The combined organics were dried (Na_2SO_4), filtered and the solvent concentrated in vacuo. The crude product was purifiedn by flash column chromatography on silica gel (eluant: EtOAc: PE = 1:1) gave the title

compound **3** as a white solid (0.68 g, 69.8%). ^{1}HNMR (400 MHz, DMSO-d_6) δ 9.43 (s, 1H), 8.24 (s, 1H), 7.29-7.34 (m, 4H), 7.21-7.25 (m, 1H), 5.76 (s, 1H), 3.44 (s, 3H), 4.29 (q, J = 7.2 Hz, 2H), 1.38 (t, J = 7.2 Hz, 3H). HRMS (ESI) m/z: 273.1203 $[M+H]^+$, calcd. for 273.1239.

3.1.4. Ethyl 6-oxo-4-(phenylamino)-1,6-dihydropyridine-3-carboxylate **(5)**

Intermediate **1a** (4.0 g, 14.5 mmol) was dissolved in a mixture of acetic acid (100 mL) and water (40 mL), and the solution was heated at reflux for 72 h. The mixture was cooled to rt, and concentrated in vacuo. The residue was purified by flash column chromatography on silica gel (eluant: CH_2Cl_2: MeOH = 100:1) gave the title compound **5** as a white solid (1.5, 41.1%). ^{1}HNMR (400 MHz, DMSO-d_6) δ 9.36 (s, 1H), 9.15 (s, 1H), 8.25 (s, 1H), 7.27-7.33 (m, 4H), 7.20-7.25 (m, 1H), 5.75 (s, 1H), 4.24 (q, J = 7.2 Hz, 2H), 1.37 (t, J = 7.2 Hz, 3H). HRMS (ESI) m/z: 259.1042 $[M+H]^+$, calcd. for 259.1083.

3.1.5. 6,7-dimethoxy-4-(4-nitrophenoxy)quinoline **(7a)**

4-Nitrophenol (12.5 g, 89.6 mmol) was added into a suspension of 4-chloro-6,7-dimethoxyquinoline (10.0 g, 44.8 mmol) in PhCl (80 mL). The resulting mixture was stirred at reflux for 16 h. The solvent was evaporated under reduced pressure, and the residue was dissolved in CH_2Cl_2 (150 mL) The solution was washed by 10% NaOH aqueous solution (3×30 mL), water (30 mL) and dried ($MgSO_4$), and evaporated to obtain the title compound as a yellow solid (9.6 g, 65.7%) without further purification. HRMS (ESI) m/z: 327.0949 $[M+H]^+$, calcd. for 327.0981.

3.1.6. 4-((6,7-dimethoxyquinolin-4-yl)oxy)aniline **(8a)**

A mixture of **7a** (9.6 g, 29.4 mmol), Fe (8.2 g, 0.15 mol) and AcOH (0.5 mL) in 90% EtOH (100 mL) was refluxed with vigorous agitation for 4 h. The hot solution was filtered through celite and the filter cake was washed with hot EtOH (20 mL). The combined filtrate was concentrated under reduced pressure to afford a dark brown solid, which was recrystallized from EtOH to afford **8a** as yellow solid (7.2 g, 82.9%). HRMS (ESI) m/z: 297.1205 $[M+H]^+$, calcd. for 297.1239.

3.1.7. General Procedure for the synthesis of target compounds **9a-b, 10a-l** and **11-14**

A solution of acid (0.6 mmol), DIPEA (0.75 mmol), HATU (0.6 mmol) and aniline (0.5 mmol) was stirred at rt in DMF (2 mL) for 4 h. The solvent was poured into ice water (6 mL), and the crude product was isolated by filtration. After purification on silica gel (eluant: EtOAc: PE = 1:1), the desired adducts were obtained.

N-(4-((6,7-dimethoxyquinolin-4-yl)oxy)phenyl)-6-oxo-4-(phenylamino)-1,6-dihydropyridine-3-carboxamide **(9a)**. Yield 60.8%. White solid. ^{1}HNMR (400 MHz, DMSO-d_6) δ 11.49 (br, 1H), 10.37 (s, 1H), 9.64 (s, 1H), 8.48 (d, J = 5.2 Hz, 1H), 8.12 (s, 1H), 7.78 (d, J = 12.0 Hz, 2H), 7.52 (s, 1H), 7.40-7.44 (m, 3H), 7.26-7.29 (m, 4H), 7.16-7.19 (m, 1H), 6.46 (d, J = 5.2 Hz, 1H), 5.64 (s, 1H), 3.95 (s, 3H), 3.94 (s, 3H). HRMS (ESI) m/z: 509.1802 $[M+H]^+$, calcd. for 509.1825.

N-(4-((6,7-dimethoxyquinolin-4-yl)oxy)phenyl)-1-methyl-6-oxo-4-(phenylamino)-1,6-dihydropyridine-3-carboxamide **(9b).** Yield 64.3%. White solid. ^{1}HNMR (400 MHz, DMSO-d_6) δ 10.38 (s, 1H), 9.45 (s, 1H), 8.48 (d, J = 5.2 Hz, 1H), 8.46 (s, 1H), 7.77-7.80 (m, 2H), 7.52 (s, 1H), 7.39-7.44 (m, 3H), 7.26-7.31 (m, 4H), 7.15-7.18 (m, 1H), 6.46 (d, J = 5.2 Hz, 1H), 5.74 (s, 1H), 3.95 (s, 3H), 3.94 (s, 3H), 3.43 (s, 3H). HRMS (ESI) m/z: 523.1971 $[M+H]^+$, calcd. for 523.1981.

6-chloro-N-(4-((6,7-dimethoxyquinolin-4-yl)oxy)phenyl)-4-(phenylamino)nicotinamide **(10a).** Yield 57.7%. White solid. ^{1}HNMR (400 MHz, DMSO-d_6) δ 10.69 (s, 1H), 9.82 (s, 1H), 8.67 (s, 1H), 8.50 (d, J = 5.2 Hz, 1H), 7.81-7.91 (m, 2H), 7.54 (s, 1H), 7.46-7.49 (m, 2H), 7.42 (s, 1H), 7.31-7.38 (m, 4H), 7.23-7.29 (m, 1H), 6.91 (s, 1H), 6.48 (d, J = 5.2 Hz, 1H), 3.97 (s, 3H), 3.96 (s, 3H). HRMS (ESI) m/z: 527.1432 $[M+H]^+$, calcd. for 527.1486.

6-chloro-N-(4-((6,7-dimethoxyquinolin-4-yl)oxy)phenyl)-4-((3-fluorophenyl)amino)nicotinamide **(10b).** Yield 64.1%. ^{1}HNMR (400 MHz, DMSO-d_6) δ 10.69 (s, 1H), 9.81 (s, 1H), 8.65 (s, 1H), 8.49 (d, J = 5.2 Hz, 1H), 7.84-7.87 (m, 2H), 7.52 (s, 1H), 7.43-7.49 (m, 1H), 7.40 (s, 1H), 7.29-7.33 (m, 2H) , 7.22-7.26 (m, 1H), 7.19-7.21 (m, 1H), 7.04-7.07 (m, 1H), 7.03 (s, 1H), 6.46 (d, J = 5.2 Hz, 1H), 5.64 (s, 1H), 3.95 (s, 3H), 3.94 (s, 3H). HRMS (ESI) m/z: 545.1366 $[M+H]^+$, calcd. for 545.1392.

6-chloro-N-(4-((6,7-dimethoxyquinolin-4-yl)oxy)phenyl)-4-((4-

fluorophenyl)amino)nicotinamide **(10c).** Yield 61.9%. White solid. ^{1}HNMR (400 MHz, DMSO-d_6) δ 10.68 (s, 1H), 9.69 (s, 1H), 8.67 (s, 1H), 8.49 (d, *J* = 5.2 Hz, 1H), 7.84-7.87 (m, 2H), 7.51 (s, 1H), 7.44-7.48 (m, 1H), 7.41 (s, 1H), 7.29-7.32 (m, 2H) , 7.22-7.26 (m, 1H), 7.18-7.21 (m, 1H), 7.04-7.08 (m, 1H), 7.03 (s, 1H), 6.46 (d, *J* = 5.2 Hz, 1H), 5.64 (s, 1H), 3.95 (s, 3H), 3.94 (s, 3H). HRMS (ESI) m/z: 545.1405 $[M+H]^+$, calcd. for 545.1392.

6-chloro-N-(4-((6,7-dimethoxyquinolin-4-yl)oxy)phenyl)-4-((2-fluorophenyl)amino)nicotinamide **(10d).** Yield 65.6%. ^{1}HNMR (400 MHz, DMSO-d_6) δ 10.72 (s, 1H), 9.79 (s, 1H), 8.69 (s, 1H), 8.50 (d, *J* = 5.2 Hz, 1H), 7.86-7.89 (m, 2H), 7.52-7.56 (m, 2H), 7.37-7.41 (m, 2H), 7.28-7.36 (m, 4H), 6.68 (m, 1H), 6.49 (d, *J* = 5.2 Hz, 1H), 3.96 (s, 3H), 3.95 (s, 3H). HRMS (ESI) m/z: 545.1371 $[M+H]^+$, calcd. for 545.1392.

6-chloro-4-((2-chlorophenyl)amino)-N-(4-((6,7-dimethoxyquinolin-4-yl)oxy)phenyl)nicotinamide **(10e).** Yield 67.3%. White solid. ^{1}HNMR (400 MHz, DMSO-d_6) δ 10.72 (s, 1H), 10.05 (s, 1H), 8.73 (s, 1H), 8.48 (d, *J* = 5.2 Hz, 1H), 7.84-7.88 (m, 2H), 7.59-7.64 (m, 2H), 7.52 (s, 1H), 7.29-7.32 (m, 3H), 6.79 (s, 1H), 6.47 (d, *J* = 5.2 Hz, 1H), 3.95 (s, 3H), 3.94 (s, 3H). HRMS (ESI) m/z: 561.1013 $[M+H]^+$, calcd. for 561.1096.

6-chloro-4-((3-chlorophenyl)amino)-N-(4-((6,7-dimethoxyquinolin-4-yl)oxy)phenyl)nicotinamide **(10f).** Yield 62.6%. White solid. ^{1}HNMR (400 MHz, DMSO-d_6) δ 10.68 (s, 1H), 9.76 (s, 1H), 8.64 (s, 1H), 8.49 (d, *J* = 5.2 Hz, 1H), 7.84-7.87 (m, 2H), 7.52 (s, 1H), 7.42-7.47 (m, 2H), 7.40 (s, 1H), 7.24-7.34 (m, 4H), 6.98 (s, 1H), 6.47 (d, *J* = 5.2 Hz, 1H), 3.95 (s, 3H), 3.94 (s, 3H). HRMS (ESI) m/z: 561.1018 $[M+H]^+$, calcd. for 561.1096.

6-chloro-4-((4-chlorophenyl)amino)-N-(4-((6,7-dimethoxyquinolin-4-yl)oxy)phenyl)nicotinamide **(10g).** Yield 61.9%. White solid. ^{1}HNMR (400 MHz, DMSO-d_6) δ 10.67 (s, 1H), 9.75 (s, 1H), 8.64 (s, 1H), 8.48 (d, *J* = 5.2 Hz, 1H), 7..87 (d, J = 8.8 Hz, 2H), 7.52 (s, 1H), 7.47 (d, *J* = 8.8 Hz, 2H), 7.40 (s, 1H), 7.38 (d, *J* = 8.8 Hz, 2H), 7.32 (d, *J* = 8.8 Hz, 2H), 6.92 (s, 1H), 6.45 (d, *J* = 5.2 Hz, 1H), 3.95 (s, 3H), 3.94 (s, 3H). HRMS (ESI) m/z: 561.1048 $[M+H]^+$, calcd. for 561.1096.

4-((2-bromophenyl)amino)-6-chloro-N-(4-((6,7-dimethoxyquinolin-4-

yl)oxy)phenyl)nicotinamide **(10h).** Yield 69.6%. White solid. ^{1}HNMR (400 MHz, DMSO-d_6) δ 10.68 (s, 1H), 9.75 (s, 1H), 8.63 (s, 1H), 8.49 (d, J = 5.2 Hz, 1H), 7.84-7.87 (m, 2H), 7.52-7.55 (m, 2H), 7.38-7.40 (m, 4H), 7.29-7.32 (m, 2H), 6.96 (s, 1H), 6.45 (d, J = 5.2 Hz, 1H), 3.95 (s, 3H), 3.94 (s, 3H). ^{13}CNMR (100 MHz, DMSO-d_6) δ 165.6, 160.4, 153.6, 153.1, 152.5, 150.7, 150.5, 149.8, 149.3, 146.9, 140.6, 136.4, 131.9, 128.3, 126.2, 123.0 (2C), 122.7, 122.4, 121.8 (2C), 115.6, 114.9, 108.3, 107.1, 103.6, 99.6, 56.2 (2C). HRMS (ESI) m/z: 605.0570, 607.0544 $[M+H]^+$, calcd. for 605.0591, 607.0571.

4-((3-bromo-4-fluorophenyl)amino)-6-chloro-N-(4-((6,7-dimethoxyquinolin-4-yl)oxy)phenyl)nicotinamide **(10i).** Yield 64.8%. White solid. ^{1}HNMR (400 MHz, DMSO-d_6) δ 10.73 (s, 1H), 9.77 (s, 1H), 8.69 (s, 1H), 8.50 (br, 1H), 7.73-7.86 (m, 3H), 7.32-7.50 (m, 6H), 6.76 (s, 1H), 6.47 (br, 1H), 3.95 (s, 6H). ^{13}CNMR (100 MHz, DMSO-d_6) δ 165.8, 160.4, 153.8, 153.1, 152.7, 150.8, 150.6, 149.8, 149.3, 146.9, 136.3, 128.8, 128.0, 123.2 (2C), 121.8 (2C), 120.5, 120.4, 115.6, 114.3, 108.3, 107.1, 103.6, 99.5, 56.2 (2C). HRMS (ESI) m/z: 623.0490, 625.0477 $[M+H]^+$, calcd. for 623.0497, 625.0477.

4-((4-bromo-2-fluorophenyl)amino)-6-chloro-N-(4-((6,7-dimethoxyquinolin-4-yl)oxy)phenyl)nicotinamide **(10j).** Yield 66.0%. White solid. ^{1}HNMR (400 MHz, DMSO-d_6) δ 10.70 (s, 1H), 9.96 (s, 1H), 8.63 (br, 2H), 7.89 (br, 2H), 7.36-7.58 (m, 7H), 6.86 (s, 1H), 6.58 (br, 1H), 3.98 (s, 6H). HRMS (ESI) m/z: 623.0495, 625.0482 $[M+H]^+$, calcd. for 623.0497, 625.0477.

6-chloro-N-(4-((6,7-dimethoxyquinolin-4-yl)oxy)phenyl)-4-(naphthalen-1-ylamino)nicotinamide **(10k).** Yield 54.9%. White solid. ^{1}HNMR (400 MHz, DMSO-d_6) δ 10.74 (s, 1H), 10.18 (s, 1H), 8.72 (s, 1H), 8.49 (d, J = 5.2 Hz, 1H), 8.04 (m, 1H), 7.89-7.93 (m, 4H), 7.61-7.63 (m, 4H), 7.53 (s, 1H), 7.41 (s, 1H), 7.33 (m, 2H), 6.49 (d, J = 5.2 Hz, 1H), 3.95 (s, 3H), 3.94 (s, 3H). HRMS (ESI) m/z: 577.1658 $[M+H]^+$, calcd. for 577.1643.

4-((3-bromo-4-fluorophenyl)amino)-6-chloro-N-(4-((6,7-dimethoxyquinolin-4-yl)oxy)-3-fluorophenyl)nicotinamide **(10l).** Yield 61.8%. ^{1}HNMR (400 MHz, DMSO-d_6) δ 10.82 (s, 1H), 9.62 (s, 1H), 8.62 (s, 1H), 8.51 (d, J = 5.2 Hz, 1H), 7.95-7.99 (m, 1H), 7.69 (m, 1H), 7.61 (m, 1H), 7.43-7.56 (m, 5H), 6.86 (s, 1H), 6.47 (d, J = 5.2 Hz, 1H), 3.97 (s, 6H). HRMS (ESI) m/z:

641.0339, 643.0323 $[M+H]^+$, calcd. for 641.0403, 643.0382.

6-bromo-4-((3-bromo-4-fluorophenyl)amino)-N-(4-((6,7-dimethoxyquinolin-4-yl)oxy)-3-fluorophenyl)quinoline-3-carboxamide **(11).** Yield 63.1%. White solid. ^{1}HNMR (400 MHz, DMSO-d_6) δ 10.73 (s, 1H), 9.63 (s, 1H), 8.62 (s, 1H), 8.51 (d, J = 5.2 Hz, 1H), 8.27 (s, 1H), 8.17 (m, 1H), 8.11 (m, 1H), 7.59 (m, 1H), 7.41-7.53 (m, 6H), 6.86 (s, 1H), 6.47 (d, J = 5.2 Hz, 1H), 3.95 (s, 3H), 3.94 (s, 3H). HRMS (ESI) m/z: 735.0012, 737.0015. $[M+H]^+$, calcd. for 735.0054, 737.0034.

2-((3-bromo-4-fluorophenyl)amino)-N-(4-((6,7-dimethoxyquinolin-4-yl)oxy)-3-fluorophenyl)nicotinamide **(12).** Yield 66.4%. White solid. ^{1}HNMR (400 MHz, DMSO-d_6) δ 10.85 (s, 1H), 10.20 (s, 1H), 8.50 (d, J = 5.2 Hz, 1H), 8.41 (m, 1H), 8.29-8.31 (m, 1H), 8.24-8.27 (m, 1H), 8.00-8.04 (m, 1H), 7.66-7.69 (m, 1H), 7.60-7.64 (m, 1H), 7.56 (s, 1H), 7.51 (t, J = 8.8 Hz, 1H), 7.43 (s, 1H), 7.32 (t, J = 8.8 Hz, 1H), 7.00-7.03 (m, 1H), 6.47 (d, J = 5.2 Hz, 1H), 3.97 (s, 6H). HRMS (ESI) m/z: 607.0733, 609.0718 $[M+H]^+$, calcd. for 607.0792, 609.0772.

4-((3-bromo-4-fluorophenyl)amino)-2-chloro-N-(4-((6,7-dimethoxyquinolin-4-yl)oxy)-3-fluorophenyl)-6-methylnicotinamide **(13).** Yield 63.7%. White solid. MS (ESI) m/z: 655.0 $[M+H]^+$. ^{1}HNMR (400 MHz, DMSO-d_6) δ 10.63 (s, 1H), 9.67 (s, 1H), 8.49 (d, J = 5.2 Hz, 1H), 7.93-7.97 (m, 1H), 7.68 (m, 1H), 7.63 (m, 1H), 7.43-7.54 (m, 5H), 6.85 (s, 1H), 6.48 (d, J = 5.2 Hz, 1H), 3.95 (s, 6H), 2.61 (s, 3H). HRMS (ESI) m/z: 655.0521, 657.0502 $[M+H]^+$, calcd. for 655.0559, 657.0539.

3.2. Kinase Assay [30]

All target compounds were tested for their inhibitory rate (@ 0.2 μM) against Aur A and Aur B by mobility shift assay. Dilute the compounds to 500 mM by DMSO, then transfer 10 mL of compound to a 96-well plate as the intermediate plate, add 90 μL kinase buffer to each well. Transfer 5 μL of each well of the intermediate plate to 384-well plates. Kinase base buffer, FAM-labeled peptide, ATP and enzyme solution were added. Wells containing the substrate, enzyme, DMSO without compound were used as DMSO control. Wells containing just the substrate without enzyme were used as low control. Incubate at room temperature for 10 min. Add 10 μL

peptide solution to each well. Incubate at 28 ℃ for specified period of time and stop reaction by 25 μL stop buffer. At last collect data on Caliper program (Perkin Elmer, US) and convert conversion values to inhibition values.

3.3. MTT assay [26]

Taking Cabozantinb as positive control, the *in vitro* cytotoxic activity of target compounds was evaluated with SW620, HT-29, NCI-H1975 and Hela cancer cell lines by the colorimetric MTT assay. Briefly, the cancer cell lines were cultured in DMEM (Hyclone®) or RPMI 1640 (Hyclone®) supplement with 10% fetal bovine serum (FBS) as well as 1% (v/v) penicillin and streptomycin. Cells were incubated in 96-well plates at a density of 6×10^3 cells/well and incubated in 5% CO_2 at 37 ℃ for 24 h. DMSO content was less than 0.1%. Then, the cells were exposed to various concentrations of tested compounds and the cell cultures were continued for another 72 h. Subsequently, 10 μL of fresh MTT (5 mg/mL) was added to each well and incubated with cell at 37 ℃ for 4 h. The medium was replaced with 100 μL of DMSO to dissolve the formed formazan crystals, and the absorbency at 492 nm (for absorbance of MTT formazan) and 630 nm (for the reference wavelength) was measured with the ELISA reader. The IC_{50} values were calculated by using GraphPad Prism 5.0.

3.5. IncuCyte live-cell imaging assays [30]

SW620 cancer cells were incubated in 96-well plates at a density of 5×10^3 cells/well and incubated in a tissue culture incubator at 37 ℃ and 5% CO_2 in an IncuCyte (Essen BioScience). The cells were cultured for 24 h, and different concentration of compound **10i**, **10l** (10.0, 3.33, 1.11, 0.37 or 0.12 μg/mL) and Cabozantinib (10.0, 3.33, 1.11 or 0.37 μg/mL) were added. Assay was performed according to the manufacturer's protocol. All samples consisted of three replicates. Images were captured by 10 times mirror every 1 h over or 84 h monitor proliferation and cytotoxicity, and 48 h for apoptosis. Red and green fluorescent signals were measured, and red-fluorescent cells and green-fluorescent cells were counted as dead cells and apoptotic cells, respectively.

4. Conclusions

In summary, a series of nicotinamide derivatives were synthesized, evaluated for their biological activities, and SAR was illustrated preliminarily. 4-((3-Bromo-4-fluorophenyl)amino)-6-chloro-*N*-(4-((6,7-dimethoxyquinolin-4-yl)oxy)-3-fluorophenyl)nicotinamide **(10l)** was identified as the most potent inhibitor of Aur A. In addition, compound **10l** showed excellent antitumor activity against SW620 and NCI-H1975 with IC_{50} values were 0.61 and 1.06 μM, respectively. As a potent antitumor agent, **10l** performed excellent apoptosis, antiproliferation and cytotoxicity against SW620 cells in a dose- and time-dependent manner. More compounds were being synthesized by our group and biological evaluation was also ongoing, including kinase profiles, cell cycle arrest and inhibition of kinase phosphorylation, *etc*. In addition, improving water-solubility and kinase selectivity are also main contents in the following work.

Acknowledgments

This work was supported by the National Natural Science Foundation of China (21562053) and Science and Technology Foundation of Guizhou Province (Qian Ke He J Zi [2014]2181).

References

[1] Noble, M.E.; Endicott, J.A.; Johnson, L.N. Protein kinase inhibitors: insights into drug design from structure. Science, 2004, 303: 1800−1805.

[2] Gautschi, O.; Heighway, J.; Mack, P.C.; Purnell, P.R.; Lara, P.N., Jr.; Gandara, D.R. Aurora kinases as anticancer drug targets. Clin. Cancer Res., 2008, 14: 1639−1648.

[3] Carmena, M.; Earnshaw, W.C. The cellular geography of aurora kinases. Nat Rev Mol Cell Biol., 2003, 4:842–854.

[4] Carmena, M.; Earnshaw, W.C. The cellular geography of aurora kinases. Nature Rev. Mol. Cell Biol., 2003, 4: 842−854.

[5] Fu, J.; Bian, M.; Jiang, Q.; Zhang, C. Roles of Aurora kinases in mitosis and tumorigenesis. Mol. Cancer Res., 2007, 5: 1−10.

[6] Nigg, E.A. Mitotic kinases as regulators of cell division and its checkpoints. Nat Rev Mol

Cell Biol., 2001, 2: 21–32.

[7] Vader, G.; Lens, S.M. The Aurora kinase family in cell division and cancer. Bioch Biophy Acta., 2008, 1786:60–72.

[8] Barr, A.R.; Gergely, F. Aurora-A: the maker and breaker of spindle poles. Cell Sci., 2007, 120: 2987–2996.

[9] Saeki, T.; Ouchi, M.; Ouchi, T. Physiological and oncogenic Aurora – a pathway. Int J Biol Sci., 2009, 5: 758–762.

[10] Vader, G.; Medma, R.H.; Lens, S.M.A. The chromosomal passenger complex: guiding Aurora-B through mitosis. J Cell Biol., 2006, 173 (6): 833–837.

[11] Carmena, M.; Ruchaud, S.; Earnshaw, W.C. Making the Auroras glow: regulation of Aurora A and B kinase function by interacting proteins. Curr. Opin. Cell. Biol., 2009, 21: 796−805.

[12] Sasai, K.; Katayama, H.; Stenoien, D.L.; Fujii, S.; Honda, R.; Kimura, M.; Okano, Y.; Tatsuka, M.; Suzuki, F.; Nigg, E.A.; Earnshaw W.; Brinkley, W.R.; Sen, S. Aurora-C kinase is a novel chromosomal passenger protein that can complement Aurora-B kinase function in mitotic cells. Cell Motil Cytoskelet., 2004, 59: 249–263.

[13] Sarvagalla, S.; Coumar, M.S. Structural biology insight for the design of sub-type selective Aurora kinase inhibitors. Curr. Cancer Drug Targets, 2015, 15(5), 375-393.

[14] Borisa, A.C.; Bhatt, H.G. A comprehensive review on Aurora kinase: Small molecule inhibitors and clinical trial studies. European Journal of Medicinal Chemistry, 2017, 140: 1-19.

[15] Gorgun, G.; Calabrese, E.; Hideshima, T.; Ecsedy, J.; Perrone, G.; Mani, M.; Ikeda, H.; Bianchi, G.; Hu, Y.; Cirstea, D.; Santo, L.; Tai, Y.-T.; Nahar, S.; Zheng, M.; Bandi, M.; Carrasco, R.D.; Raje, N.; Munshi, N.; Richardson, P.; Anderson, K.C. A novel Aurora-A kinase inhibitor MLN8237 induces cytotoxicity and cell-cycle arrest in multiple myeloma. Blood, 2010, 115: 5202−5213.

[16] Manfredi, M.G.; Ecsedy, J. A.; Chakravarty, A.; Silverman, L.; Zhang, M.; Hoar, K.M.; Stroud, S.G.; Chen, W.; Shinde, V.; Huck, J.J.; Wysong, D.R.; Janowick, D.A.; Hyer, M.L.;

LeRoy, P.J.; Gershman, R.E.; Silva, M.D.; Germanos, M.S.; Bolen, J.B.; Claiborne, C.F.; Sells, T.B. Characterization of alisertib (MLN8237), an investigational smallmolecule inhibitor of Aurora A kinase using novel in vivo pharmacodynamic assays. Clin. Cancer Res., 2011, 17: 7614−7624.

[17] Fancelli, D.; Moll, J.; Varasi, M.; Bravo, R.; Artico, R.; Berta, D.; Bindi, S.; Cameron, A.; Candiani, I.; Cappella, P.; Carpinelli, P.; Croci, W.; Forte, B.; Giorgini, M.L.; Klapwijk, J.; Marsiglio, A.; Pesenti, E.; Rocchetti, M.; Roletto, F.; Severino, D.; Soncini, C.; Storici, P.; Tonani, R.; Zugnoni, P.; Vianello, P. 1,4,5,6-Tetrahydropyrrolo[3,4-c]pyrazoles: identification of a potent Aurora kinase inhibitor with a favorable antitumor kinase inhibition profile. J. Med. Chem., 2006, 49: 7247−7251.

[18] Borges, K.S.; Andrade, A.F.; Silveira, V.S.; Marco Antonio, D.S.; Vasconcelos, E. J.R.; Antonini, S.R.R.; Tone, L.G.; Scrideli, C.A. The aurora kinase inhibitor AMG 900 increases apoptosis and induces chemosensitivity to anticancer drugs in the NCI-H295 adrenocortical carcinoma cell line. Anti-Cancer Drugs, 2017, 28: 634–644.

[19] Linardopoulos, S.; Blagg, J. Aurora Kinase Inhibition: A New Light in the Sky?. J. Med. Chem., 2015, 58: 5186−5188.

[20] Pinkerton, A.B.; Sergienko, E.; Bravo, Y.; Dahl, R.; Ma, C.; Sun, Q.; Jackson, M.R.; Cosford, N.D.P.; Millán, J.L. Discovery of 5-((5-chloro-2-methoxyphenyl)sulfonamido)nicotinamide (SBI-425), a potent and orally bioavailable tissue-nonspecific alkaline phosphatase (TNAP) inhibitor. Bioorganic & Medicinal Chemistry Letters, 2018, 28: 31–34.

[21] Gao, X.; Liu, L.; Liu, H.; Tang, J.; Kang, L.; Wu, H.; Cui, P.; Yan, J. Structure–activity relationship investigation of benzamide and picolinamide derivatives containing dimethylamine side chain as acetylcholinesterase inhibitors. Journal of Enzyme Inhibition and Medicinal Chemistry, 2018, 33 (1): 110–114.

[22] Felts, A.S.; Rodriguez, A.L.; Blobaum, A.L.; Morrison, R.D.; Bates, B.S.; Gray, A.T.; Rook, J.M.; Tantawy, M.N.; Byers, F.W.; Chang, S.; Venable, D.F.; Luscombe, V.B.; Tamagnan,

G.D.; Niswender C.M.; Daniels, J.S.; Jones, C.K.; Conn, P.J.; Lindsley, C.W.; Emmitte, K.A. Discovery of *N*-(5-Fluoropyridin-2-yl)-6-methyl-4-(pyrimidin-5-yloxy)picolinamide (VU0424238): A Novel Negative Allosteric Modulator of Metabotropic Glutamate Receptor Subtype 5 Selected for Clinical Evaluation. J. Med. Chem. 2017, 60, 5072−5085.

[23] El-Damasy, A.K.; Seo, S.H.; Cho, N.; Kang, S.B.; Pae, A.N.; Kim, F.; Keum, G. Design, synthesis, in-vitro antiproliferative activity and kinase profile of new picolinamide based 2-amido and ureido quinoline derivatives. European Journal of Medicinal Chemistry. 2015, 101: 754-768.

[24] Zeidan, M.A.; Mostafa, A.S.; Gomaa, R.M.; Abou-zeid, L.A.; El-Mesery, M.; El-Sayed, M.A.; Selim, K.B. Design, synthesis and docking study of novel picolinamide derivatives as anticancer agents and VEGFR-2 inhibitors. European Journal of Medicinal Chemistry, 2019, 168: 315-329.

[25] Qi, B.; Mi, B.; Zhai, X.; Xu, Z.; Zhang, X.; Tian, Z.; Gong, P. Discovery and optimization of novel 4-phenoxy-6,7-disubstituted quinolines possessing semicarbazones as c-Met kinase inhibitors. Bioorganic & Medicinal Chemistry, 2013, 21: 5246–5260.

[26] Qi, B.; Yang, Y.; He, H.; Yue, X.; Zhou, Y.; Zhou, X.; Chen, Y.; Liu, M.; Zhang, A.; Wei, F. Identification of novel N^1-(2-aryl-1, 3-thiazolidin-4-one)-N^3-aryl ureas showing potent multi-tyrosine kinase inhibitory activities. European Journal of Medicinal Chemistry, 2018, 146: 368-380.

[27] Spicer, J.A.; Rewcastle, G.W.; Kaufman, M.D.; Black, S.L.; Plummer, M.S.; Denny, W.A.; Quin, J.; Shahripour, A.B.; Barrett, S.D.; Whitehead, C.E.; Milbank, J.B.J.; Ohren, J.F.; Gowan, R.C.; Omer, C.; Camp, H.S.; Esmaeil, N.; Moore, K.; Sebolt-Leopold, J.S.; Pryzbranowski, S.; Merriman, R.L.; Ortwine, D.F.; Warmus, J.S.; Flamme, C.M.; Pavlovsky, A.G.; Tecle, H. 4-Anilino-5-carboxamido-2-pyridone Derivatives as Noncompetitive Inhibitors of Mitogen-Activated Protein Kinase Kinase, J. Med. Chem. 2007, 50, 5090-5102.

[28] Zhu, M.; Qui, Z.; Hiel, G. P.; Sieberth, S. M. Photocycloaddition of four-carbon-tethered pyridones. Intramolecular hydrogen bonding and facilitated amide hydrolysis by a proximal

secondary alcohol. J. Org. Chem. 2002, 67, 3487-3493.

[29] Mekheimer, R. A. Fused quinoline heterocycles I. First example of the 2,4-diazido-quinoline-3-carbonitrile and 1-aryl-1,5-dihydro-1,2,3,4,5,6- hexaazaacephenanthrylene ring systems. J. Chem. Soc., Perkin Trans. 1 1999, 2183-2188.

[30] Qi, B.;Yang, Y.; Gong G.; He, H.; Yue, X.; Xu, X.; Hu Y.; Li, J.; Chen, T.; Wan, X.; Zhang, A.; Zhou, G. Discovery of N^1-(4-((7-(3-(4-ethylpiperazin-1-yl)propoxy)-6-methoxyquinolin-4-yl)oxy)-3,5-difluorophenyl)-N^3-(2-(2,6-difluorophenyl)-4-oxothiazolidin-3-yl)urea as a multi-tyrosine kinase inhibitor for drug-sensitive and drug-resistant cancers treatment. European Journal of Medicinal Chemistry, 2019, 163:10-27.

Graphical Abstract